Investigation on the Limit State of a Triple-column Spar Floating Wind Turbine Concept

Liang Li [a], *Jin Wang* [b,c]

a. Department of Naval Architecture, Ocean and Marine Engineering, University of Strathclyde, Glasgow, UK

b. COTEC Offshore Engineering Solutions, Houston, Texas, USA

c. School of Naval Architecture, Ocean and Civil Engineering, Shanghai Jiao Tong University, Shanghai, China

ABSTRACT

The limit state of a newly proposed floating wind turbine concept, in terms of ultimate structural load and fatigue damage load, is studied in the present work. This novel floating structure utilizes a triple-column spar platform to support the wind turbine. An aero-hydro-servo-elastic numerical model is developed to simulate its coupled dynamics. The probability distribution of the ultimate structural load is estimated based on the Monte-Carlo method. In order to reduce computation endeavor, a statistic model is used to extrapolate the sampled-based distribution function. The S-N curve method, a state-of-art fatigue analysis approach, is used to assess the fatigue damage load. The limit states of tower base and fairlead are investigated. It is shown that the newly proposed triple-column spar concept suffers less fatigue damage and the ultimate structural loads are also reduced, resulting in the enhancement of safety level of the floating wind turbine system.

KEY WORDS: floating wind turbine; triple-column spar; limit state; ultimate structural load, fatigue damage.

INTRODUCTION

Powered by the increasing global pursuit of sustainable energy, the traditional wind industry is moving to deeper water to exploit high-quality offshore wind resources. Since the successful deployment of the world's first floating wind turbine concept, Hywind demo (Equinor, 2017), various floating structures have been developed for offshore floating wind turbine application. Principle Power proposed the WindFloat (Principle Power, 2015), a semisubmersible floating wind turbine. Three types of floating wind turbine concept are designed in the OC4 DeepCwind project (Koo et al., 2014). More recently, Li and Wang (2019) investigated the long-term extreme loads of a new concept triple-column spar-type floating wind turbine, or TC Spar. The TC Spar is designed to be self-installed, thus no need for costly large DP crane vessels to perform offshore installation. Another advantage of the TC Spar is that the smaller diameter hull column makes it easier for efficient standardized fabrication.

In advance of the practical application of a new floating wind turbine concept, the structural integrity and reliability must be carefully investigated. Usually, the ultimate limit state and fatigue limit state are two critical parameters to assess the reliability and safety of the structure. Cheng et al. (2017) compared the extreme structural response of a horizontal axis floating wind turbine and a vertical axis floating wind turbine. Hu et al. (2016) developed an integrated structural strength analysis method for a spar type floating wind turbine. Inertia and wave-induced loads were addressed with a quasi-static method and the wind force was dealt with a static approach. Li et al. (2019a) discussed the limitation of the classic environmental contour method in the application to offshore wind turbines. A modified approach was proposed to estimate extreme loads. Michailides et al. (2016) examined the response of a combined wind/wave energy concept in extreme environmental conditions with both experimental and numerical methods. Liu et al. (2017) studied the aerodynamic damping effect on offshore wind turbine tower loads and different aerodynamic damping models were used. Li et al. (2019b) studied the nonlinear short-term extreme responses of a spar type floating wind turbine in turbulent wind.

Fatigue is the weakening of a material caused by cyclic loading that results in progressive and localized structural damage and the growth of cracks. Li et al. (2018a) investigated the fatigue analysis for the tower base of a spar-type wind turbine. Marino et al. (2017) investigated the fatigue loads of a floating wind turbine with both linear and nonlinear wave models. Graf et al. (2016) used the Monte Carlo approach to evaluate the long-term fatigue loads of a floating wind turbine. Li et al. (2018b) calculated the fatigue load of a hybrid offshore renewable energy system.

The present study reports a preliminary investigation on the feasibility of a recently proposed triple-column spar floating wind turbine, in terms of ultimate limit state and fatigue limit state. This paper is organized as: Firstly, a brief introduction of the triple-column floating wind turbine is given. This paper subsequently interprets the numerical analysis model and the methodologies used to assess the ultimate and fatigue limit states. Numerical simulations are conducted to investigate the ultimate structural load and fatigue damage. A comparison between the present triple-column spar and a classic single-column spar is also given. Finally, conclusions drawn from the present research are presented.

MODEL DESCRIPTION

Fig. 1 sketches the hull of the triple-column spar platform considered in the present study. As shown, the new concept is made up of three columns with a radius of 2.4 m to produce the buoyancy force. The three columns are connected with two discs, one of which is above the still sea

level and acts as the deck to mount the wind turbine. The main dimensions are listed in Table 1. The NREL 5MW baseline wind turbine (Jonkman et al. 2009), a three-blade upwind wind turbine, is adopted to produce electrical power from offshore wind. The hub height is 90 m above the still water level and the rotor radius is about 63 m. Please refer to (Jonkman et al. 2009) for more details of the wind turbine configuration.

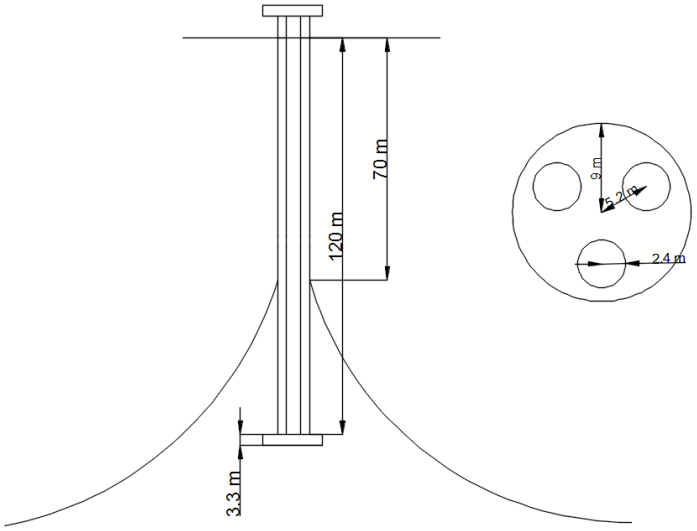

Fig. 1. Triple-column spar concept.

Table 1 Main dimensions of the triple-column spar.

Item	Value
Draft	123.3 m
Volume	7354 m^3
Mass	6.78×10^6 kg
CoG	(0 m, 0 m, -100 m)
I_{xx}	1.24×10^{10} kg·m^2
I_{yy}	1.24×10^{10} kg·m^2
I_{zz}	1.64×10^{8} kg·m^2

The triple-column concept is displaced at sea site with a water depth of 320 m and moored by three slack catenary lines. The fairleads are connected to the platform at 70 m below the still water level. The three lines are oriented at 60°, 180°, and 300° about the vertical axis. The relevant properties of the mooring line are listed in Table 2.

Table 2 Mooring line properties.

Item	Value
Depth to anchors	320 m
Depth of fairleads	70 m
Radius to anchors	853.87 m
Radius to fairleads	6.4 m
Unstretched mooring line length	902.2 m
Mooring line diameter	0.09 m
Equivalent mooring line mass density	77.71 kg/m
Equivalent mooring line extensional stiffness	3.84×10^5 kN

ANALYSIS METHODOLOGY

Numerical Model

The aero-hydro-servo-elastic coupled simulation code FAST (Jonkman and Buhl Jr, 2005) developed by the National Renewable Energy Laboratory (NREL) is used to simulate the dynamic performance of the triple-column spar floating wind turbine.

Assuming that the wave fluid is ideal, the wave-structure is addressed in the framework of potential flow theory. The wave radiation force is calculated with the convolution term to consider the free surface memory effect. All the hydrodynamic coefficients (added mass, wave force transfer function, etc.) that to be inputted into FAST are first obtained using boundary element analysis program Wadam (DNV, 1994). The boundary element model of the platform is sketched in Fig. 2, where a total of 10134 elements are generated.

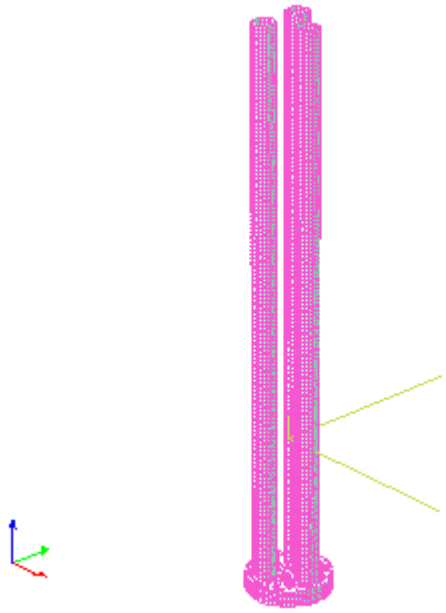

Fig. 2 Boundary element model of the platform.

The blade element momentum (BEM) method is used to compute the wind force acting on the rotor. The blade is separated into a set of elements, and the interactions between neighboring elements are neglected. By seeking the so-called induced velocity, the aerodynamic load on each element is determined using the lift and drag coefficients of the airfoil. For an offshore floating wind turbine, both the platform motions and wind turbulence produce unsteadiness of the inflow seen by the rotor. The unsteady effect is accounted for using the dynamic wake model developed by Minnema (1998), which can be regarded as a correction to the induced velocity determined by the BEM method.

A variable-speed torque controller and a blade pitch controller are incorporated into the wind turbine. The variable-speed torque controller is active in below-rated operational state. The control algorithm is to maximize the power output by adjusting the rotor speed while the blade pitch angle is fixed at zero. On the contrary, the blade-pitch controller works in above-rated state to regulate generator power by increasing the pitch angle of the blade.

Ultimate Load

The ultimate load is estimated using the mean up-crossing rate method. It is assumed that the random number of up-crossing can be approximated by the Poisson distribution. The distribution of extreme value y_{max} of the load $y(t)$ over time interval $[0, T]$ is thus described as

$$P(y_{\max} \le y) = \exp\left(-\int_0^T v^+(y,t)dt\right) \quad (1)$$

where $v^+(y,t)$ is the up-crossing rate corresponding to load level y. In this circumstance, the probability of y_{max} exceeding load level y is given by

$$P(y_{\max} > y) = 1 - \exp\left(-\hat{v}^+(y)T\right)$$
$$\hat{v}^+(y) = \frac{1}{T}\int_0^T v^+(y,t)dt \quad (2)$$

The mean up-crossing rate $\hat{v}^+(y)$ can be easily obtained from the time series of the signal that is about to analyze. For example, if we have k independent realizations of the random process and let $n_j^+(y,T)$ denote the number of up-crossings in realization j, then the sample-based mean up-crossing rate is given by

$$\hat{v}^+(y) \approx \overline{v}^+(y)$$
$$\overline{v}^+(y) = \frac{1}{kT}\sum_{j=1}^{k} n_j^+(y,T) \quad (3)$$

Eq. (3) is the classic approach to estimate the mean up-crossing rate $\hat{v}^+(y)$ through Monte-Carlo method. If the defined level y is not very high, then just a few simulation realizations of the random process will produce satisfactory approximation. Nevertheless, extensive simulations are required to evaluate the extreme value in the tail region. To save computation resource, the extrapolation method proposed by Naess and Gaidai (2008) is used in this study to extrapolate the sample-based mean up-crossing rate. The extrapolation method is based on the observation of marine structures so that it is applicable in this study. The mean up-crossing rate is approximated by

$$\overline{v}^+(y) \approx v_{fit}^+(y)$$
$$v_{fit}^+(y) = q \cdot \exp\left\{-a(y-b)^c\right\}, y \geq y_0 \quad (4)$$

where q, a, b and c are all constant values. y_0 is the lower limit of the sampled data used for the extrapolation. In the present research, the extrapolated up-crossing rate is based on 40 independent numerical realizations ($k = 40$). y_0 = (mean+std) is used, where 'mean' is the average mean response of the 40 numerical realizations; 'std' is the average standard deviation of the 40 numerical realizations. To put emphasis on the more reliable sampled data, the weight factor proposed by Naess and Gaidai (2009) is used here

$$\Theta = \sum_{j=1}^{N} w_j \left|\log\left(\overline{v}^+(y_j)\right) - \log(q) + a(y_j - b)^c\right|^2 \quad (5)$$

where Θ is the mean square error; $w_j = \left|\log(CI_+(y_j)) - \log(CI_-(y_j))\right|^{-2}$ is the weight factor. And,

$$CI_{\pm}(y) = \overline{v}^+(y) \pm \frac{1.96 s(y)}{\sqrt{k}}$$
$$s^2(y) = \frac{1}{k-1}\sum_{j=1}^{k}\left(\frac{n_j^+(y,T)}{T} - \overline{v}^+(y)\right)^2 \quad (6)$$

The least square optimization method is used to get q, a, b and c by minimizing Θ.

Fatigue Damage Load

Wind, wave and inertial loads applied at certain structural components cause fluctuation leading to fatigue damage. The fatigue analysis is performed with MLife (MLife, 2017). The S-N method is used to evaluate the fatigue damage caused by fluctuating load. The fluctuating load is broken down into individual hysteresis cycles by matching local minima with local maxima in the time series, which is characterized by a load-mean and range. It is assumed that the damage accumulates linearly with each of these cycles according to Miner's Rule. In this case, the overall damage rate produced by all the cycles is given by

$$DR = \sum_i \frac{n_i}{N_i(L_i^{RF})} / T$$
$$N_i(L_i^{RF}) = \left(2 \cdot \frac{L^{ult} - \left|L^{MF}\right|}{\left(L_i^{RF}\right)}\right)^m \quad (7)$$

n_i is the damage count, N_i is the number of cycles to failure, L^{RF} is the cycle's load range corresponding to the fixed load-mean L^{MF}, L^{ult} is the design load resistance of the structure and m is the Wholer exponent. The Wholer exponent is selected based on DNV design standard (DNV, 2010). Considering the shape of the tower base and mooring line, the B1 S-N curve is selected. Within the B1 category, the 'air' group and 'sea water' group is selected for the tower base and the mooring line, respectively. T is the simulation time length.

SIMULATION RESULTS

The environmental conditions considered in the present research is given in Table 3. The random wave is specified by the JONSWAP wave spectrum. Head wind and wave are modelled for each 1-hr numerical simulation, and the simulation time discretization is 0.0125 s. Comparison with a classic spar floating wind turbine, OC3-Hywind (Jonkman, 2010), is presented to demonstrate the advantage of the triple-column spar platform.

Table 3 Environmental conditions

Wind speed	Hs (m)	Tp (s)	Shape factor
11.4 m/s	6	10	3.3

Due to the stochastic feature of the ocean wave, a large number of independent numerical realizations are required to investigate the limit state of the triple-column spar offshore floating wind turbine. This subsection conducts a convergence study on the numbers of numerical realizations. Table 4 shows the sensitivity of response standard deviations to the sample sizes. Hereinafter, the results presented are based on 40 independent numerical realizations.

Table 4 Standard deviations of structural response

No.	Tower base bending moment	Fairlead tension
10	21,233 kN·m	11.85 kN
20	21,204 kN·m	11.62 kN
30	21,058 kN·m	11.57 kN
40	21,042 kN·m	11.53 kN

Hydrodynamic Coefficients

Fig. 3 illustrates the wave excitation force transfer function for surge and pitch modes, respectively. Regardless of the wave frequency, the triple-column spar is subject to fewer wave loads in pitch mode. Meanwhile, the surge wave forces exerting on the triple-column spar is generally lower within the typical wave frequency range. The reduction of wave load is due to two factors. First, the volume of TC_spar is 8% smaller than that of Hywind. Also, the radius of three columns of TC_spar and the distance between them have been optimized to acquire appropriate hydrodynamic interaction, which reduces the wave load as well. Since the triple-column spar platform is exposed to lower levels of wave loads in the oceans, it can be expected to have a reduced dynamic response compared with the Hywind single column spar concept.

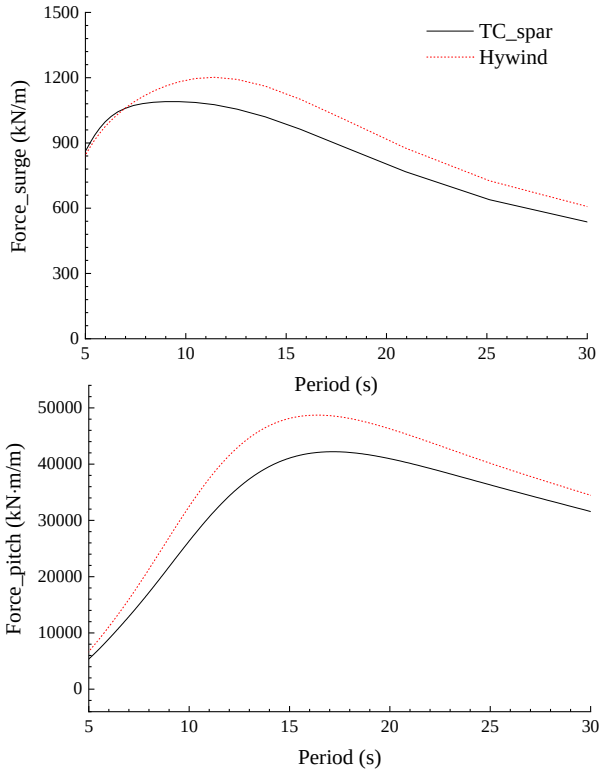

Fig. 3. Wave excitation transfer function.

Structural Response

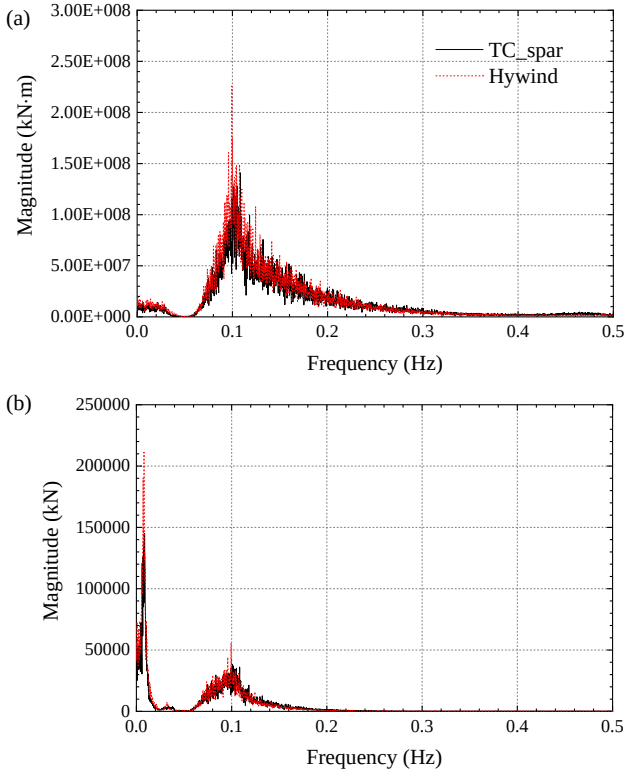

Fig. 4. FFT analysis of structural loads. (a) tower base fore-aft bending moment; (b) mooring line tension force.

Fig. 4 present the FFT (fast Fourier transform) of the structural loads at the tower base and mooring fairlead. For the tower base bending moment, two response peaks are observed. The major response peak is excited at 0.1 Hz, namely the wave peak period. The major peak is mainly induced by the inertial motion of the platform. In addition, a minor response peak is seen at low-frequency range, due to the low-frequency platform surge motion. Although the fairlead tension force is also excited at the wave peak frequency and low frequency, respectively, the low-frequency response dominates the fairlead tension. This is because the fairlead tension is mainly governed by the platform surge motion whilst the tower base bending moment mainly by platform pitch motion. It is easy to find that the structural loads are reduced when the triple-column spar platform is used. It implies that the triple column floating wind turbine is less to exceed its limit state.

Ultimate Load

To assess the risk level of the floating wind turbine, the ultimate structural loads at the tower base and fairlead are investigated. The extrapolated mean up-crossing rate based on 40 independent 1-hr numerical realizations is used to represent the extremal loads. Fig. 5 plots the mean up-crossing rate of the tower base fore-aft bending moment and fairlead tension force, respectively. For the period of 1 hour, the mean up-crossing rate of 10^{-5} gives a probability of exceedance of approximately 3%. Hereinafter, the load level corresponding to 10^{-5} is used as the extreme structural load.

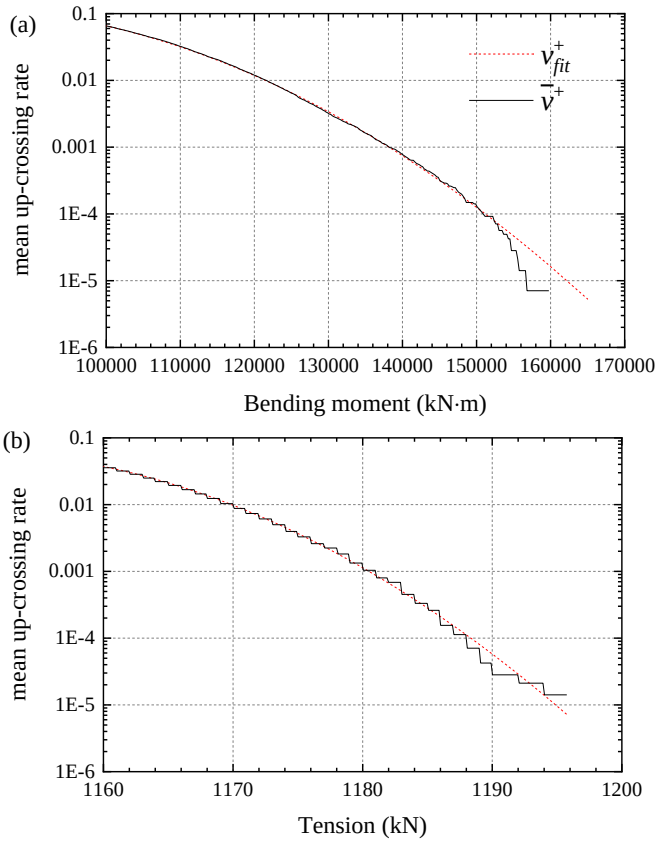

Fig. 5. Mean up-crossing rate of extreme structural load (TC_spar). (a) tower base bending moment; (b) mooring line tension force.

Table 5 compares the extreme structural loads of the triple-column spar and the Hywind. Although the extreme fairlead tension force is not reduced much, the extreme tower base bending moment is reduced by 10% with the usage of the triple-column spar platform.

Table 5 Extreme structural loads

	Tower base bending moment	Fairlead tension
Triple-column spar	162,000 kN·m	1195 kN
Hywind	177,000 kN·m	1227 kN

Fatigue Damage

Due to the cyclic load, the fracture may happen before the structure exceeds its design ultimate load. Although the tower is subject to both axial stress and shear stress, the shear stress has a much smaller influence on the limit state as suggested by Kvittem and Moan (2015). As shown in Fig. 6, the axial stress at the reference point is calculated as

$$\sigma = \frac{N_z}{A} + \frac{M_y}{I_y} r \tag{8}$$

where N_z is the axial force; A is the nominal cross section area; M_y is bending moment respectively; I_y is the sectional second moment of the area.

For the mooring line, the axial stress is assumed uniform across the section and simplified as

$$\sigma = \frac{N_z}{A} \tag{9}$$

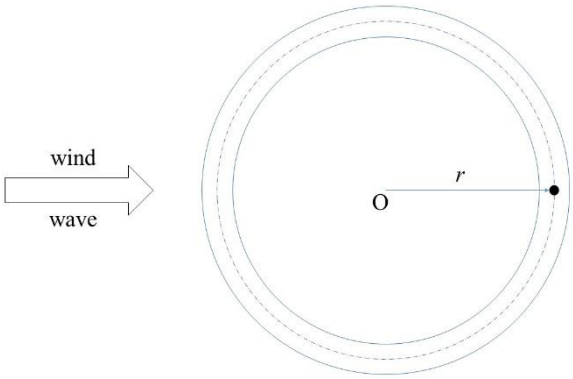

Fig. 6. Top view of tower base section.

Fig. 7 demonstrates the load cycle counts of tower base stress and fairlead tension stress, respectively. The load cycles are counted using the rain-flow algorithm, according to the ASTM E1049 standard (ASTM International, 2017). It is found that, within low stress range, the load cycles account more rapidly when the triple-column spar platform is used. Nevertheless, the load cycles are reduced within the high stress range. Considering that the structure is much more sensitive to high amplitude load cycles, the triple-column floating wind turbine is subject to less fatigue damage.

The fatigue damage rates of tower base and fairlead are shown in Table 6. Compared with the fairlead tension force, the tower base bending moment has a much higher damage rate. It indicates tower base is a critical structural connection point. According to Table 6, the fatigue damage rates of the triple–column spar floating wind turbine are lower than those of the Hywind, manifesting that the triple-column floating wind turbine is subject to less fatigue damage. From the fatigue point of view, the triple-column floating wind turbine has a longer lifetime.

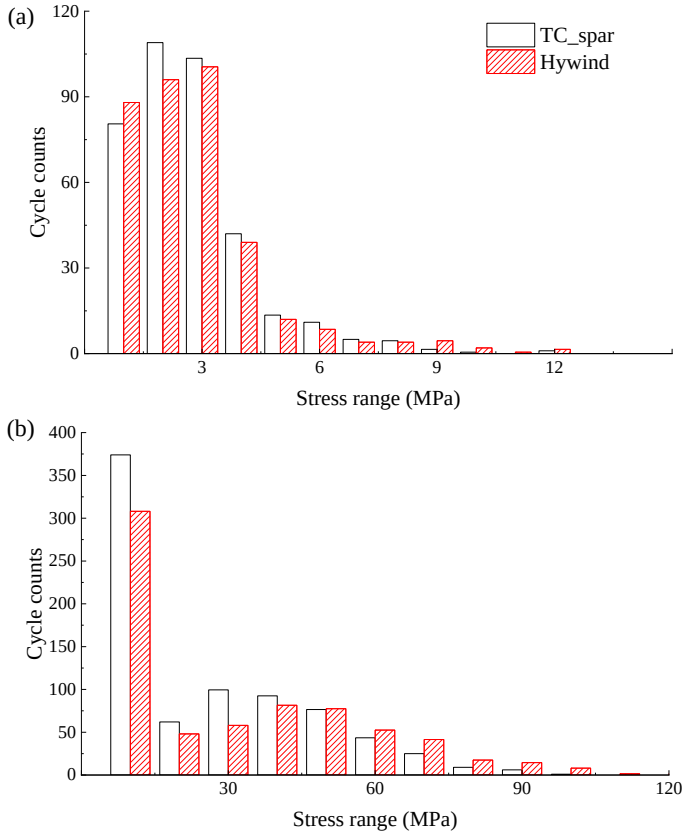

Fig. 7 Load cycle counts. (a) mooring line; (b) tower base

Table 6 Fatigue damage rate

	Tower base bending moment	Fairlead tension
Triple-column spar	7.54×10^{-6}	5.60×10^{-9}
Hywind	1.25×10^{-5}	8.52×10^{-9}

CONCLUSIONS

The ultimate and fatigue limit states of a triple-column spar floating wind turbine are investigated in this study. The mean up-crossing method is used to estimate extreme responses. The size of simulation realizations is reduced by an extrapolation method, which approximates the mean up-crossing rate in the tail region. The cumulative fatigue damage rate is calculated based on the S-N method. A comparative study between the present concept and a classic spar floating wind turbine is conducted.

The stochastic responses of tower base fore-aft bending moment and mooring line tension force under the joint action of wind and wave are simulated. The tower base bending moment and fairlead tension force are reduced, with the usage of the triple-column spar platform.

Based on the extrapolated mean up-crossing rate, the extreme values of the stochastic responses are estimated. The maximum fore-aft bending moment of the triple-column spar is smaller than that of a classic single-column spar.

The cumulative damage rate is used to indicate the short-term fatigue damage caused to the structural component. It is shown that the tower base has a smaller probability of failure for the triple-column spar-type floating wind turbine concept.

REFERENCES

ASTM International, (2017). Standard Practices for Cycle Counting in Fatigue Analysis.

Cheng, ZS, Madsen, HA, Chai, W., Gao, Z., Moan, T., (2017). "A comparison of extreme structural responses and fatigue damage of semi-submersible type floating horizontal and vertical axis wind turbines," *Renew Energ* 108, 207-219.

DNV, 2010. Fatigue design of offshore steel structures, No. DNV-RP-C203.

DNV, 1994. WADAM—Wave Analysis by Diffraction and Morison Theory.

Equinor, 2017. Hywind—the world's leading floating offshore wind solution, https://www.equinor.com/en/what-we-do/hywind-where-the-wind-takes-us.html.

Graf, PA, Stewart, G, Lackner, M, Dykes, K, Veers, P, (2016). "High-throughput computation and the applicability of Monte Carlo integration in fatigue load estimation of floating offshore wind turbines," *Wind Energy* 19 (5), 861-872.

Hu, ZQ, Liu, Y, Wang, J, (2016). "An integrated structural strength analysis method for Spar type floating wind turbine," *China Ocean Eng* 30 (2), 217-230.

Jonkman, J, Buterfield, S, Musial, W, Scott, G, 2009. Definition of a 5-MW Reference Wind Turbine for Offshore System Development. National Renewable Energy Laboratory (NREL).

Jonkman, J, 2010. Definition of the Floating System for Phase IV of OC3. National Renewable Energy Laboratory (NREL)..

Jonkman, J, Buhl Jr, ML, 2005. FAST User's Guide. National Renewable Energy Laboratory (NREL).

Koo, BJ, Goupee, AJ, Kimball, RW, Lambrakos, KF, (2014. "Model Tests for a Floating Wind Turbine on Three Different Floaters". *J Offshore Mech Arct* 136 (2), 020907.

Kvittem, MI, Moan, T, (2015). "Time domain analysis procedures for fatigue assessment of a semi-submersible wind turbine," *Mar Struct* 40, 38-59.

Li, L, Yuan, ZM, J, CY, Gao, Y, (2018a). "Ultimate structural and fatigue damage loads of a spar-type floating wind turbine," *Ships and Offshore Strucutres* 14(6) 582-588

Li, L, Cheng, ZS, Yuan, ZM, Gao, Y, (2018b). "Short-term extreme response and fatigue damage of an integrated offshore renewable energy system," *Renew Energ* 126, 617-629.

Li, L, Wang, J, (2019). "Long-Term Extreme Structural Loads of a Triple-Column Spar Floating Wind Turbine Concept," *Proc 29th Int Offshore and Polar Eng Conf*, Honolulu, Hawaii, ISOPE.

Li, L, Yuan, ZM, Gao, Y, Zhang, XS, Tezdogan, T, (2019a). "Investigation on long-term extreme response of an integrated offshore renewable energy device with a modified environmental contour method," *Renew Energ* 132 33-42.

Li, L, Liu, YC, Yuan, ZM, Gao, Y, (2019b). " Dynamic and structural performances of offshore floating wind turbines in turbulent wind flow," *Ocean Eng* 179, 92-103.

Liu, X, Lu, C, Li, GQ, Godbole, A, Chen, Y, (2017). "Effects of aerodynamic damping on the tower load of offshore horizontal axis wind turbines," *Appl Energ* 204, 1101-1114.

MLife, 2017. https://nwtc.nrel.gov/MLife/.

Marino, E, Giusti, A, Manuel, L, (2017). "Offshore wind turbine fatigue loads: The influence of alternative wave modeling for different turbulent and mean winds," *Renewa Energ* 102, 157-169.

Michailides, C, Gao, Z, Moan, T, (2016). "Experimental and numerical study of the response of the offshore combined wind/wave energy concept SFC in extreme environmental conditions," *Mar Struct* 50, 35-54.

Minnema, JE, (1998). "Pitching moment predictions on wind turbine blades using the Beddoes-Leishman model for unsteady aerodynamics and dynamic stall," Department of Mechanical Engineering, University of Utah.

Naess, A, Gaidai, O, (2008). "Monte Carlo methods for estimating the extreme response of dynamical systems," *J Eng Mech* 134 (8), 628-636.

Naess, A, Gaidai, O, (2009). "Estimation of extreme values from sampled time series," *Struct Saf* 31 (4), 325-334.

Principle Power, 2015. WindFloat, http://www.principlepowerinc.com/en/windfloat.